Energy, Mines and Resources Canada
Énergie, Mines et Ressources Canada

CANMET
Canada Centre for Mineral and Energy Technology
Centre canadien de la technologie des minéraux et de l'énergie

LITERATURE REVIEW ON FRACTURE TOUGHNESS TESTING OF THE HEAT-AFFECTED-ZONE

J.T. McGrath

DECEMBER 1976

MINERALS RESEARCH PROGRAM
PHYSICAL METALLURGY RESEARCH LABORATORIES
CANMET REPORT 77-59

Available by mail from:

Printing and Publishing
Supply and Services Canada,
Ottawa, Canada K1A 0S9

CANMET
Energy, Mines and Resources Canada,
555 Booth St.,
Ottawa, Canada K1A 0G1

or through your bookseller.

Catalogue No. M38–13/77-59 Price: Canada: $1.75
ISBN 0-660-01582-X Other countries: $2.10

Price subject to change without notice.

En vente par la poste:

Imprimerie et Édition
Approvisionnements et Services Canada,
Ottawa, Canada K1A 0S9

CANMET
Énergie, Mines et Ressources Canada,
555, rue Booth
Ottawa, Canada K1A 0G1

ou chez votre libraire.

Nº de catalogue M38-13/77-59 Prix: Canada: $1.75
ISBN 0-660-01582-X Autres pays: $2.10

Prix sujet à changement sans avis préalable.

FOREWORD

This review of fracture toughness testing methods suitable for assessing the fracture toughness of heat-affected zones (HAZ) of weldments has been carried out by the Canadian Welding Development Institute, Toronto, Ontario, Canada. It was performed in part fulfilment of contracts SQ 15.23440-1073 and SQ 17.23440-6-9002 entitled "Research on Heat-Affected Zone Toughness of Welded Joints in Microalloy Steel" and was funded by the Department of Energy, Mines and Resources, Ottawa, Canada.

W.A. Gow,
Director, Minerals Research Program

AVANT-PROPOS

Cette étude des méthodes d'essai de ductilité à la cassure qui permettent d'évaluer ténacité des zones thermiquement affectées de piéces soudées a été réalisée par le Canadian Welding Development Institute de Toronto (Ontario). Elle a été effectuée dans le cadre de l'exécution d'une partie des contrats SQ 15.23440-1073 et SQ 17.23440-6-9002 intitulés "Research on Heat-Affected Zone Toughness of Welded Joints in Microalloy Steel" et fut financée par le ministère de l'Energie, des Mines et des Ressources d'Ottawa (Canada).

W.A. Gow,
Directeur, Programme de recherche sur les minéraux

LITERATURE REVIEW ON FRACTURE TOUGHNESS TESTING OF THE HEAT-AFFECTED-ZONE

by

J.T. McGrath*

ABSTRACT

The literature on the evaluation of the fracture toughness of the heat-affected zone (HAZ) of weldments has been reviewed.

Several aspects related to HAZ toughness determination were addressed. It was indicated that HAZ toughness should be related to crack initiation rather than to crack propagation because cracks which initiate in the HAZ seldom remain there during the propagation stage of fracture. The fracture mechanics techniques available for measuring fracture toughness related to crack initiation can be selected on the basis of the amount of elastic-plastic deformation. For example, when linear elastic behaviour prevails, the K_{IC} test applies. If general yielding takes place followed by abrupt fast fracture, the COD or J integral tests may be used. The Charpy test may be useful as a quality control test for comparing the HAZ toughness of various weldments provided crack initiation and propagation take place within the HAZ region. In the selection of a suitable fracture test specimen, notch location should simulate the orientation of HAZ welding defects.

A general review is given of the application of laboratory fracture toughness data to the prediction of structural failure. Costs of performing various fracture mechanics and impact tests are provided in an appendix.

---

*Canadian Welding Development Institute.

ETUDE DOCUMENTAIRE SUR LES ESSAIS DE DUCTILITE A LA CASSURE DE LA ZONE THERMIQUEMENT AFFECTEE

par

J.T. McGrath*

RESUME

L'auteur passe en revue la documentation sur l'évaluation de la ductilité à la cassure de la zone thermiquement affectée de piéces soudées.

Il traite de plusieurs aspects liés à la détermination de la ductilité de la zone thermiquement affectée. L'étude révèle que la ductilibé à la cassure d'une zone thermiquement affectée doit être liée à l'amorçage plutôt qu'à la propagation de la cassure étant donné que les fissures qui s'amorçent dans la zone thermiquement affectée y demeurent rarement au cours de la propagation de la cassure. Les essais selon la mécanique de rupture dont on dispose pour mesurer la ductilibé à la cassure associée à l'amorçage d'une fissure peuvent être choisis en fonction de l'importance de la déformation élastique et plastique. Par example, lorsqu'un matériau a tendance à afficher une déformation élastique linéaire, il faut recourir à la détermination de K_{IC}. Par contre, s'il y a dépassement général de la limite d'élasticité et rupture abrupte et rapide, on peut mesurer l'écartement critique à fond de fissure (C.O.D.) ou l'intégrale J. L'essai Charpy peut être un utile contrôle de la qualité pour comparer la ténacité de la zone thermiquement affectée de différentes pièces soudées à la condition que l'amorçage et la propagation de la fissure s'effectuent dans la zone thermiquement affectée. Lorsque l'on choisit une éprouvette pour l'essai de ductilité à la cassure, il faut que l'emplacement de l'entaille simule l'orientation des défauts de soudage de la zone thermiquement affectée.

L'auteur fait une étude générale de l'application des ténacités mesurées en laboratoire dans la prédiction des défaillances de structures. Les coûts d'exécution des essais de la mécanique de la rupture et des essais par choc sont indiqués dans une annexe.

---

*Canadian Welding Development Institute.

TABLE OF CONTENTS

TABLES

LIST OF FIGURES

INTRODUCTION

The purpose of this literature survey is to review the methods available for evaluating fracture toughness of the Heat-Affected Zone (HAZ). The survey is divided into the following sections:

1. HAZ Fracture; a discussion on whether fracture toughness should be based on crack initiation or propagation
2. Selection of Fracture Toughness Test Specimens
3. Examples of HAZ Fracture Toughness Measurement
4. Selection of Fracture Initiation Criterion; an assessment of the K_{IC}, COD, J_{IC} and K_{Id} approaches.
5. Assessment of the Charpy Test in HAZ Fracture Toughness Evaluation
6. Application of Laboratory Fracture Toughness Data in the Prediction of Structural Failure.

In any fracture toughness evaluation the economics of the various testing techniques becomes a factor. This aspect is discussed in Appendix I.

1. HAZ Fracture - An Initiation or Propagation Criterion

In evaluating fracture toughness of the HAZ of a weldment, it is important initially to decide whether fracture toughness is related to the initiation or the propagation of a crack. In a review by Munse (1) it was pointed out that, particularly in mild steel structures, no failures are reported (2) to have propagated in a weld or HAZ, i.e., cracks may initiate but they do not necessarily propagate in these regions. The reason for this behaviour is related primarily to the high residual tensile stresses which develop principally at the plate surfaces in the direction parallel to the weld centreline as illustrated in Fig. 1. In the through thickness plane of the weldment, Fig. 2, high transverse residual compressive stresses can be formed at mid-thickness. In addition to the tensile surface stresses, another factor which may discourage crack propagation, particularly in the weld metal, is the superior fracture toughness of the weld metal exhibited by mild steel weldments, (Fig. 3). The HAZ toughness can be lower than the base metal but the high component of residual tensile stress in the HAZ must discourage cracks from propagating

along the HAZ parallel to the weld centreline. Munse cites the work of Kihara et al (3), shown in Fig. 4, as an illustration of the deviation of the crack path from the weld metal/HAZ area. Consider the probability of crack propagation in the weld metal/HAZ area in weldments of high strength. Generally, the fracture toughness of weld metal, particularly in QT steels, is comparable with, and in some cases is reported to be higher than that of the base metal; thus fracture toughness is not likely to be the controlling factor in dictating a preferred path for crack propagation. However, as shown in Fig. 1, the high residual tensile stresses which develop in high strength steel weld metal/HAZ should be sufficient to restrict cracks from propagating parallel to the weld centreline in both weld metal and HAZ.

Thus, the conclusion must be that, in evaluating HAZ fracture toughness of steel weldments, a test procedure which measures crack initiation rather than crack propagation data is preferable.

2. Selection of Test Specimens

The selection of a fracture mechanics criterion (K_{IC}, COD, J_{IC}, etc.) for crack initiation in the HAZ is essential. However, of equal importance is the selection of the fracture toughness test specimen. While interpretation of fracture mechanics data may vary, the test speciment is basically one in which a notch or defect is positioned in the region of interest. The specimen is then stressed until a condition of instability is reached at the tip of the notch, with the stress and strain data leading to instability being recorded. Fracture toughness measurements in the HAZ will be meaningful only if they are made with specimens which simulate the position of welding defects in the HAZ.

2.1 Testing for Specific HAZ Cracking Problems

Before discussing the various types of specimens, the regions of the HAZ and the defects which are likely to form will be defined. The coarse-grained HAZ is the region immediately adjacent (within ~ 0.25 mm) to the fusion boundary where peak temperatures in welding exceed the A_3 temperature. The prior austenite grain size will be largest in the

coarse-grained region which is also a likely site for hydrogen-induced cold cracking, liquation cracks and reheat cracks. Next is the grain-refined HAZ. The austenite grain size is small since the temperature just exceeds the A_3. The defects present in the coarse-grained HAZ may also extend into the grain-refined HAZ. The inter-critical HAZ is a very narrow region next to the grain-refined HAZ where the maximum temperature reached during welding lies between the A_1 and A_3 temperatures.

In the sub-critical HAZ, the peak temperature is less than the A_1 temperature; thus the microstructure may be very similar to the base metal. This temperature range is such that embrittlement in the sub-critical region could take place by strain aging. However, defects that may be present in this region are not those directly related to welding, i.e., H_2 cracking, reheat cracking, etc., but may include welding-induced lamellar tearing. It is suggested that pre-existing defects such as fatigue cracks or stress corrosion cracks are more likely to be found in the sub-critical HAZ region.

The method for selecting test specimens for assessing HAZ fracture toughness is due principally to Dolby and co-workers(4). The objective in specifying test specimens has been to simulate the orientation of HAZ cracks with respect to the fusion boundary and their position with respect to the free surfaces of the welded joint. Figure 5 summarizes these specimen designs. With regard to orientation, defects will be considered which are either longitudinal or transverse to the centre-line of the weld.

Test specimens best suited to evaluating fracture toughness in weldments containing HAZ cracks longitudinal to the weld may be examined. Toe and root cracks, Fig. 6, can be induced in butt weld HAZ by hydrogen-induced cold cracking, reheat cracking or liquation cracking. The toe crack is simulated by Type 'B' specimens. The notch tip is located in the HAZ as close as possible to the coarse-grained region.

While fatigue precracking is preferred, there have been studies in which the notch has been introduced by machining a narrow slit (0.15 mm). Because of residual stresses there has been difficulty in developing a uniform fatigue crack extension in the HAZ. An adjustment factor must be applied to take account of the finite root radius of the notch in subsequent fracture toughness calculations. This will be discussed later in more detail. In simulating a root crack, Type 'B' specimens are also used with the notch introduced into the HAZ from the root face of the weldment. For toe and root cracks in fillet welds, Type 'A' specimens are recommended. The significance of lamellar tearing can be assessed by Type 'C' specimens. It is noted that there is difficulty in assessing the effect of lamellar tear type defects on fracture toughness since the distribution of inclusions at the tip of the notch may vary.

Defects which are positioned in the HAZ transverse to the weld can also be simulated. Hydrogen-induced cold cracks and reheat cracks are examples of transverse defects. This type of defect is associated mainly with butt welds. Type 'D' is suited to measure the effect of transverse defects on fracture toughness. The tip of the defect may be in the HAZ extending from the weld metal or from the base metal. In Section 3, results of fracture toughness measurements made with the two notching positions will be discussed.

The K preparation specimen (Type 'E') is a modification of Type 'B' in that a straight fusion boundary is produced and the whole of the notch tip lies within the HAZ. Since the orientation of the notch is parallel to the weld, the application of this specimen for measuring fracture toughness associated with transverse defects assumes that there is no effect of defect orientation on fracture toughness.

If a defect is present with its tip in the sub-critical region of the HAZ and subjected to thermal cycles (maximum temperature $< A_1$) during welding, embrittling due to a strain aging mechanism is possible. This type of defect would have to be present in the base metal prior to welding and is thus not commonly found. However, it will be shown in

Section 3 that such a region can have a low toughness. The specimen which simulates this situation is shown as Type 'F' in Fig. 5.

2.2 A General Approach to HAZ Fracture Toughness Testing

While it is essential to specify a fracture toughness test to assess the toughness related to a specific welding defect, it may be desirable to have a test procedure which allows for comparing of materials, processes or consumables, and general welding procedures. In the evaluation of HAZ fracture toughness it is recognized that the coarse-grained HAZ is inherently the region of lowest toughness. In a recent study by the IIW (5), it was recommended that a test specimen such as Type 'E' in Fig. 5 would fulfill the requirement of providing a representative value of HAZ fracture toughness. As an aid to selecting the position of the notch in the HAZ test specimen, it was suggested that a hardness traverse be made across the weldment to reveal the region of peak hardness. This region is usually the region of lowest toughness.

3. Examples of HAZ Fracture Toughness Measurement

In this section the measurement of fracture toughness by the specimen configurations suggested in Section 3 will be illustrated. Problems encountered in obtaining representative measurements and data interpretation will be discussed. A discussion will also be presented on the use of simulated HAZ specimen vs actual HAZ welded specimen for fracture toughness evaluation.

The work of Dolby and Saunders (6)(7) and Banks (8) reports on the measurement of fracture toughness in three regions of the HAZ:

coarse-grain region,
grain-refined region, and
sub-critical region.

In evaluating the first two, Type 'A' was used with the notch being positioned in the desired HAZ region (Fig. 5). For a range of steels investigated it was possible to distinguish the fracture toughness of the two regions from each other and from the base metal. The relative differences in toughness were related to microstructure and will not be discussed at this time. The fracture toughness of the sub-critical

region is illustrated in Fig. 7 in comparison with the base metal. This type of embrittlement, which is associated with strain aging at the notch tip, can be severe. However, it depends on a pre-existing defect being located in the base metal. This condition is expected to occur infrequently in welded structures, e.g., fatigue cracks that have not been removed completely and have been repair-welded.

The fracture toughness of the coarse-grained HAZ of C-Mn steel weldments was measured by Cane and Dolby (9). The results of the test program using a Type 'A' (Fig. 5) specimen were able to show a difference in the fracture toughness between the coarse-grained region and base metal, Fig. 8. However, in those tests where fracture initiated by ductile tearing, denoted by the open symbols in Fig. 8, there was considerable spread in the data. This illustrates the weakness of the COD test in determining critical displacement at the onset of tearing. It is obvious that the criterion of using surface displacement at maximum load to calculate δc is not sufficient. This point will be dealt with in subsequent reports when the various fracture mechanics methods are assessed.

The assessment of fracture toughness related to HAZ defects transverse to the weld was carried out in weldments of HY80 steel (10)(11). The specimen of Type 'D' in Fig. 5 was employed. The notch was positioned in two ways - (a) through the weld metal to the HAZ; and (b) through the base metal to the HAZ, as shown in Fig. 9. The results in Table 1 indicate a lower fracture toughness for the test configuration with the notch tip adjacent to the weld metal. It was suggested that the toughness of the weld metal had an influence on the magnitude of the toughness measured in the HAZ. This is possible if the plastic zone size at the tip of the notch is large enough to extend into the weld metal. If the weld metal is less tough than the HAZ, it would account for the observed low toughness in the U series specimens compared with the T series specimens. An estimate of the plastic zone size, r_y, can be made using equation 1 (12) and knowing the yield stress and an assumed value of the stress intensity factor, K_c.

$$r_y = \frac{EG}{2\pi \ \sigma ys^2} \qquad \text{Eq (1)}$$

where $EG = K_c^2$

σ_{ys} = yield stress

The significance of the plastic zone at the notch tip will be discussed later in the survey.

In another set of experiments the fracture toughness of the HAZ was measured with the notch tip perpendicular to the fusion boundary (Type 'D'; Fig. 5) and parallel to the fusion boundary (Type 'C'; Fig. 5). The base metal was a C:Mn steel plate, BS 4360, Grade 55E. The results of the tests are shown in Fig. 10. At low temperatures where cleavage was the mode of fracture, the critical COD values were similar. However, at higher temperatures (> -80°C) there was scatter in the results. For the specimen with the notch parallel to the fusion boundary, examination of the crack tip after initiation revealed that initiation took place in the weld metal and not in the HAZ. This illustrates the effect of surrounding regions on the measurement of HAZ toughness.

The value of using thermally simulated microstructure to measure HAZ toughness can be assessed by comparing toughness of simulated and weld HAZ microstructures (13). While there has been much interest in the case of simulated HAZ microstructure in evaluating toughness, it was pointed out that past work has been concerned with the use of the Charpy test in assessing toughness (13). The limitations of this test make its use questionable in monitoring fracture initiation in the HAZ; further discussion will be forthcoming. In a British Welding Institute study, simulated microstructures were produced in HY80 QT steel by using thermal cycles which matched the austenite grain size and the HAZ heating and cooling rates between weld HAZ and simulated microstructure. In this manner, the coarse-grained and grain-refined regions were studied. The COD vs temperature test results are shown in Fig. 11 and 12, along with the load values at yielding and fracture. There is little difference in

COD values for simulated and HAZ specimens, particularly for the grain-coarsened region. However, there is a noticeable difference in the load levels at yielding and fracture. This is accounted for by the author as being related to the development of plastic hinges at the notch tip during testing (13). In the HAZ specimen the plastic hinge will propagate from the HAZ of relatively high strength into base metal of lower strength resulting in a lower load at yield and fracture in comparison with the simulated specimen where such a transition does not occur. This effect of base metal on HAZ behaviour should be more apparent in the tests on the grain refined region. This was not reflected in the magnitude of the load differences but was shown in the COD results where the HAZ had a slightly higher toughness than the simulated structure. There has been limited work on the use of simulated microstructure in measuring fracture toughness associated with crack initiation. Although there are similar toughness levels indicated compared with that measured in HAZ specimen, there are indications that significant differences could result if the HAZ zone regions in question were limited in width and were affected by adjacent base metal and weld metal zones.

4. Selection of Fracture Initiation Criterion

The following fracture mechanics approaches, i.e., K_{IC}, COD, J integral and K_{Id}, may be useful in assessing the HAZ fracture toughness associated with fracture initiation. The objective will be to examine their applicability in determining HAZ toughness.

4.1 K_{IC} Test

The K_{IC} test for measuring fracture toughness was devised for materials which exhibit plane strain conditions and thus allows only a limited amount of plastic deformation to occur at the tip of a defect prior to the initiation of a state of instability leading to brittle fracture. The procedure for measuring the linear elastic fracture mechanics parameter, K_{IC}, is described in ASTM specification E399 (14) and will not be repeated here. The validity of the K_{IC} test is described by the following relationship:

$$B \geq 2.5 \left(\frac{K_{IC}}{\sigma ys}\right)^2 \qquad \text{Eq (2)}$$

where B = section thickness
σys = yield stress

This expression defines the minimum section thickness which allows the condition of plane strain to exist. In addition to the effect of section thickness, plane strain conditions can be attained by high yield stress and low service temperature.

If the HAZ of a weldment should meet the validity conditions of the K_{IC} test, the measured fracture toughness parameter can be employed to calculate the critical defect size leading to brittle fracture initiation in a structure subjected to a given applied stress. The application of fracture toughness data in the prediction of failure in full-scale structures will be discussed in Section 6.

4.2 COD Test

The COD method, as originally constituted by Wells, was intended to be applied where extensive plastic deformation at the crack tip preceded the initiation of unstable fracture (15). The procedure for measuring the critical COD level is given by the British Standards Institution (16). Briefly, in conducting the COD test, a specimen, containing a fatigue pre-crack, is loaded either in bending or tension and a force/displacement diagram is recorded as shown in Fig. 13. The critical COD (δc) is calculated from the displacement at the point of instability.

Barr et al have reviewed the force/displacement records for COD tests conducted on steels exhibiting varying amounts of plastic deformation (17). In Fig. 13(a) an unstable cleavage fracture occurred while the applied force was increasing and the critical δc was calculated from the total displacement value. Figure 13(b) illustrates the case when plastic deformation takes place prior to fracture. The plastic deformation may result in a small region of ductile crack extension followed by abrupt cleavage fracture. Once again the critical δc is calculated from maximum displacement.

When the force/displacement curve shows a region of increasing displacement under constant or reducing force as illustrated in Fig. 13(c) and 13(d), considerable ductile crack extension may initiate with final failure occurring by plastic collapse. When this occurs the COD at the onset of crack extension, δi, is taken as the critical value. If no means are available for monitoring the onset of crack extension, the British Standard allows the use of the COD at the attainment of maximum force, Sm, with the provision that this measurement be used for material comparison only (16).

The COD value, δc, can be used to determine tolerable defect size, $\bar{a}$, by the following relationship (17):

$$\bar{a} = C\left(\frac{\delta c}{ey}\right) \qquad \text{Eq (3)}$$

where ey = yield strain
C = constant

The COD test, which utilizes a small specimen, may also be useful in the prediction of the K_{IC} fracture toughness parameter. The following relation is suggested (18):

$$\delta c = \frac{\lambda K_{IC}^{2} (1 - \nu^{2})}{E(YS)} \qquad \text{Eq (4)}$$

The usefulness of this relationship will be discussed in Section 6.

4.3 J Integral

The J integral test, like the COD test, was devised to assess the fracture toughness of materials exhibiting plastic deformation prior to the initiation of a crack leading to unstable fracture. Unlike the COD test, which is concerned with events at the crack tip, the J integral provides an average measure of the elastic-plastic stress/strain field around the crack and can be used as a fracture criterion (19). The experimental procedure for measuring the J integral has been provided by Landes and Begley (20). In the technique, a bend or compace tension specimen containing a fatigue crack ($a/w \geq 0.6$) is loaded to a given displace-

ment (Fig. 14). The J value is determined from the expression

$$J = \frac{2A}{Bb} \qquad \text{Eq (5)}$$

where A = area under the load-displacement curve
B = thickness
b = uncracked ligament = W-a

The J_{IC} value associated with the onset of crack extension is obtained from the plot of J for various displacements against crack extension, Δ a, as shown in Fig. 14(d).

The potential use of the J integral test is that it can provide a K_{IC} value from a small, laboratory specimen which exhibits general yield behaviour. The critical J_{IC} is related to the critical stress intensity factor, K_{IC}, by the following equation:

$$J_{IC} = \frac{(1 - \nu^2)}{E} K_{IC}^2 \qquad \text{Eq (6)}$$

where E = Youngs modulus
ν = Poissons ratio

J_{IC} can be used to calculate K_{IC} if it meets the following proposed validity condition (21).

$$B \text{ or } W\text{-}a \geq 50 \left(\frac{J_{IC}}{\sigma ys}\right) \qquad \text{Eq (7)}$$

Examples of current research being carried out to assess the usefulness of the J integral as a fracture criterion will be given in Section 6.

It should be noted that because the J integral test is relatively recent, an ASTM procedure has yet to be approved.

4.4 K_{Id} Test

When structures are subjected to dynamic loading conditions, the appropriate stress intensity factor, K_{Id}, must be established. As with the case of static loading, there is an incentive to determine the K_{Id} value by means of a small inexpensive test specimen, particularly if the standard linear elastic fracture mechanics test requires a large specimen. The instrumented Charpy test has been developed to fulfill this requirement. This technique is well documented in two recent ASTM publications (22)(23). A test procedure for conducting an instrumented Charpy test has yet to be approved by an ASTM standard. A British specification has recently been proposed (24).

Briefly, the features of the instrumented Charpy test which makes it possible to determine the dynamic stress intensity factor K_{Id} are as follows:

(a) instrumentation allows a record of load vs time and load vs deflection;

(b) the amount of section restraint in the standard Charpy specimen (10 x 10 mm) has been increased by using a fatigue precrack. Restraint can also be increased by the use of side grooving.

(c) a range of striking velocities allows control of the strain rate.

Provided the load vs time record indicates fracture occurs before general yielding, the dynamic fracture toughness, K_{Id}, can be determined from the standard linear elastic fracture mechanics (14). The validity of the result can be determined by Equation 2.

Before the use of the dynamic instrumented impact test becomes an accepted testing technique for determining a valid K_{Id} number, investigations must be done to find out whether K_{Id} measured from the small Charpy specimen is comparable to the K_{Id} value obtained on large specimens. The results of some of these studies will be discussed in Section 6. Comments will also be made on whether dynamic fracture toughness data is required for the HAZ region of weldment.

5. Assessment of the Charpy Test in HAZ Fracture Toughness Evaluation

The usefulness of the Charpy test will be discussed under two headings:

(a) General limitations of the Charpy test

(b) Specific examples of the use of Charpy test in HAZ toughness evaluation.

5.1 Limitations of the Charpy Test

The Charpy test is an empirical test which defines the mode by which a crack will initiate and propagate under impact loading conditions. It is attractive because of its low cost and ease of testing. However, realistic design data, i.e., the ductile/brittle transition temperature, cannot be obtained from small specimens of less than full plate thickness (25). This is due primarily to the lack of mechanical restraint at the notch tip.

The most direct solution to the problem of inadequate thickness of the Charpy specimen is to increase the size of the test bar to the full thickness of the material in the actual structure. The drop-weight tear test which uses full thickness and increased fracture path, allows the attainment of a more realistic ductile/brittle transition temperature (26).

Recently, Smith and Patchett have examined methods of modifying the specimen to yield more realistic data for fracture toughness assessment (27). Essentially they modified the design to provide more section restraint. This was done by increasing notch acuity and by side grooving. The specimen depth (10 mm), notch depth (2 mm) and notched cross section (80 mm^2) were kept constant while the notch acuity and depth of side grooving were varied.

A specimen design employing a 0.15-mm wide slit notch and 2-mm deep side grooves had an NDT temperature of -40°C, in agreement with the NDT temperature as determined by a large-scale (38-mm thick) drop weight test. The results were confined to one steel composition. The amount of side grooving and degree of notch acuity will likely vary, depending on steel composition and strength.

The concept of side grooving may be useful for HAZ fracture toughness testing, by maintaining the fracture path within the HAZ.

5.2 Charpy Test as a Measure of HAZ Toughness

The use of the Charpy test in evaluating HAZ fracture toughness is questionable on the basis that it measures the energy required to initiate, as well as propagate, a crack. It was shown in Section 1 that cracks initiate in the weld metal and HAZ but tend to deflect into the parent metal during propagation.

Considering the work done using the Charpy impact test as a means of measuring the fracture toughness of (a) the HAZ of an as-welded specimen and (b) the simulated HAZ structure, Banks attempts to evaluate the fracture toughness of the coarse-grained HAZ in butt welds prepared from two structural steels of medium carbon content (0.17%), the one containing 0.024% Cb and the other < 0.001% Cb (28)(8). The welds were made by the submerged arc process. The HAZ were planar and the notch for both Charpy and COD tests at right angles to the plate surface. As shown in Fig. 15, the COD initiation transition temperature for the HAZ was greater than that for the base metal, particularly when higher heat inputs were used and the maximum HAZ grain size resulted. The Charpy results, however, indicated the HAZ to be comparable or superior in toughness to the base metal. The reason for the discrepancy is clear on examining the fractured specimens. The fracture path deviates from the HAZ region into the base metal. Thus energy absorbed during impact fracture is not totally associated with failure of the coarse-grained region of the HAZ. Similar problems in maintaining crack propagation in a specific region have been reported by Goldak and Nguyen for micro-alloy steel weldments prepared by electron beam welding, and by Taniguchi et al (29)(30).

The work of Ivens and Van den Bergh was concerned with the development of brittle microstructure in the HAZ of structural steel weldments (31)(32). The critical cooling rate for the onset of a brittle microstructure was established by the Charpy test. The only problem in obtaining meaningful results occurred when fast cooling rates (Δt < 5 to 10 seconds in

cooling from 800° to 500°C) produced a narrow brittle zone in the HAZ which was not easily detectable by impact testing.

The Charpy test was shown to be successful in distinguishing the difference in fracture toughness for the various regions of the HAZ in weld simulated specimens (33)(34). Schofield and Weiner used induction heating to produce an 8-mm wide zone of uniform structure in 10-mm square specimens (33). The coarse-grained, fine-grained and inter-critical regions of the HAZ were simulated and tested by both the Charpy and COD techniques. The materials tested were a variety of C/Mn steels, some containing micro-alloy additions of Cb and V. The Charpy results showed a similar trend in fracture toughness to the COD results. The fracture toughness values of the fine-grained and inter-critical regions of the HAZ were comparable or superior to those of the base material. The worst toughness properties were exhibited by the coarse-grained region of the HAZ. The same trends were found by Grover and Jolley for simulated HAZ in a low alloy structural steel (34).

6. Application of Laboratory Fracture Toughness Data in Prediction of Structural Failure

The present section discusses the fracture mechanics techniques and their usefulness in predicting the failure of materials which fracture by various modes, ranging from cleavage to plastic collapse.

6.1 K_{IC} Data

Provided linear elastic conditions exist in an engineering structure, e.g., a heavy-walled pressure vessel, the laboratory measured value of K_{IC} should provide an accurate determination of the critical defect size leading to initiation of fast fracture (35)(36)(37). However, accuracy of the predicted defect size will depend on the ability to measure the applied stress. If the section of the structure being assessed is the HAZ, then the magnitude of the residual stress must be included in the applied stress. The appropriate K expression related to type of defect (surface, embedded, or through thickness) must also be selected. Finally, the laboratory measured K_{IC} must have been determined under the

environmental conditions, i.e., temperature, irradiation, etc., which the structure would encounter in service.

6.2 COD Data

The application of COD test data can take two forms:

(a) the direct prediction of critical defect size or applied stress leading to unstable fracture in materials exhibiting general yield,

(b) the calculation of a K_{IC} value from small-scale COD tests when the testing of large-scale specimens becomes impractical.

In dealing first with the direct prediction of structural failure, the work of Kirby et al (38) describes the correlation between small-scale COD tests and large-scale vessel and wide plate tests. Ductility was controlled by the test temperature. This was selected in such a way that failure occurred without prior visible tearing or extension, not unlike that depicted in Fig. 13(a) and 13(b). Figure 16 shows moderate agreement between the critical COD, δc, values measured for wide plate, vessel and bend test specimens, with the bend test values tending to be lower than those obtained in the large-scale tests. The failure stresses of the wide plate and pressure vessels compare reasonably well with the failure stresses predicted by the COD bend tests, as shown in Fig. 17. The following equations were employed to calculate failure stress -- Equation 8 for wide plate and Equation 9 for pressure vessel.

$$\delta = \frac{8\ \sigma y.a}{\pi.E} \cdot \ln \sec \left(\frac{\pi}{2} \cdot \frac{\sigma}{\sigma y}\right) \qquad (8)$$

$$\delta = \frac{8\ \sigma y.a}{\pi.E} \left[\ln \sec \left(\frac{\pi}{2} \cdot \frac{\sigma H}{\sigma y}\right)\right] \left(1+1.61\ \frac{a^2}{Rt}\right) \qquad (9)$$

Equation 9 contains a factor, $(1+1.61\ \frac{a^2}{Rt})$, which allows for bulging taking place in the vessel wall.

COD tests carried out where ductile tearing occurred prior to failure, Fig. 13(c) and 13(d), resulted in a high degree of conservatism regarding prediction of vessel failure (39). Figure 18 shows the critical COD results measured for a pressure vessel and a laboratory bend specimen. The δc value for the vessel was measured at the onset of rapid tearing.

Some slow crack extension preceded this event. The δc value for the bend test was calculated for the displacement at maximum load. For δc values > 0.02 - 0.03 in. (0.5 - 0.75 mm), the COD for vessel and bend specimens differed by more than a factor of two. One can conclude that the COD approach is not applicable in cases where failure takes place by ductile tearing and plastic collapse.

The potential use of small-scale COD test specimens for determining K_{IC} data when large-scale specimens are impractical, has been investigated (18). The objective of the study was to determine the dependence of the critical COD value (δc) on specimen thickness. Unless the geometry independence of δc can be established, an accurate calculation of K_{IC} through a relationship such as Equation 3 is not possible. The steel (HY80) which Griffis (18) investigated exhibited ductile crack extension with a force displacement diagram of the form shown in Figure 13(d). He measured the COD at initiation (δi) and at maximum load (δm). Figures 19 and 20 indicate the effect of specimen size on the two types of critical COD value. The COD associated with initiation was unchanged at thickness, B < 1 cm. However, for B > 1 cm there was a continued rise in COD with a possible leveling off at B > 4.5 cm. The plot of COD at maximum load in Fig. 20 indicates a sharp change in COD for B > 1 cm. The work of Fearnehough et al (40) reported the change in COD at initiation and maximum load as a function of ligament depth (W-a) for four steels of varying strength and composition. The results were in many respects similar to the findings of Griffis. The COD at maximum load increased continuously for W-a $\leq$ 10 cm. However, the COD at initiation remained constant for w-a > 3 cm for three of the four steels investigated. The conclusion is that the COD (δm) at maximum load, because of its dependence on specimen geometry, is not acceptable for the calculation of K_{IC}. The COD (δi) associated with the initiation of crack extension, may be useful in calculating K_{IC}, provided it can be shown to be independent of specimen geometry.

6.3 J Integral Data

The potential application of the J integral test is the calculation of a K_{IC} value from small-scale, often fully plastic, laboratory specimens. The J integral test can only be useful in this regard if it can be shown that the critical J_{IC} value associated with crack initiation is independent of specimen geometry. In a recent investigation of the fracture properties of an intermediate steel, the J integral test indicated considerable plastic deformation very similar to that shown by the COD test in Fig 13(d)(18). From a series of load-displacement tests, the critical J value was determined at initial crack extension and at maximum load. The plot of J integral at the onset of crack extension against specimen size in Fig. 21 indicated the critical J value to be constant when the B or W-a dimension increased beyond 1.5 cm. This is in agreement with the proposed validity criterion, Equation 7. The critical J value at maximum load was dependent upon specimen geometry as shown in Figure 20. In another study, Landes and Begley reported good agreement between K_{IC} calculated from J_{IC} for crack extension and K_{IC} measured (19). J_{IC} values were determined from 1-in. thick compact tension specimens of ASTM A216-C steel. J_{IC} values were converted to K_{IC} numbers using Equation 6. Valid K_{IC} values were measured, using 12-in. thick specimens.

Although more investigations are required, the evidence indicates that J_{IC} value associated with the onset of crack extension can be useful in calculating a valid K_{IC} number without resorting to the expense of a linear elastic fracture mechanics test employing a large test specimen.

6.4 K_{Id} Data

If the K_{Id} value determined from an instrumented Charpy test is to be a useful parameter in the prediction of structural failure, it must be comparable to the K_{Id} determined from a large specimen. If such a comparison is to be made, it should be done under the same conditions of temperature and strain rate. Weiss et al carried out K_{Id} tests on instrumented Charpy specimens and large precracked bend specimens over a range of temperatures and strain rates for 17-7 PH stainless steel (41). The results are shown in Fig. 22.

There was reasonable agreement between the K_{Id} values for small and large specimens at a strain rate of $10°$/sec. This strain rate was obtained in the Charpy test by a striking velocity of 100 mm/sec. At the higher strain rate of 10^2/sec. there was a significant difference between the K_{Id} of the Charpy test and the large specimen. Unfortunately, it was not possible to obtain data for the large specimens at the high strain rate and extrapolated results had to be used.

Tetelman and Server used precracked Charpy specimens of A533 B steel to obtain data of K_{Id} and compared with K_{Id} from the dynamic testing of large compact tension specimens (42). The K_{Id} data showed good agreement between the small and large specimens, but unfortunately the tests were not carried out under the same strain rate conditions.

One can conclude from this work that there is still some doubt as to whether an acceptable K_{Id} value can be obtained from a precracked Charpy specimen. One can also make a general comment on whether dynamic K_{Id} data should be a requirement for the HAZ region. The fact has already been discussed that cracks can initiate in the HAZ. Once initiated, a crack tends to deflect from the HAZ into the base material. Crack propagation in the base material represents a condition of dynamic loading. Thus, there is a justification for K_{Id} data to be available for the base material. Since extensive crack propagation does not occur in the HAZ, there is less justification for K_{Id} data for this region.

7. Conclusions

The following general comments can be made on the evaluation of the fracture toughness of the HAZ:

1. Fracture toughness of the HAZ should be based on a crack initiation rather than crack propagation criterion.

2. In the selection of a fracture toughness test specimen, the specimen notch should be located in such a manner as to simulate the position of specific welding defects. Fatigue precracking is the preferred technique for introducing the notch.

3. For a general evaluation of HAZ fracture toughness, the notch should be located in the region with potentially the lowest toughness, i.e., the coarse-grained region.

4. Test specimens with simulated HAZ microstructure are useful for distinguishing the relative differences between the various HAZ regions. The toughness values determined by simulated and actual HAZ specimens are comparable. However, significant differences could result if the actual HAZ regions were narrow and affected by the adjacent base metal and weldmetal zones.

5. The selection of a fracture mechanics technique for measuring the fracture associated with crack initiation is dependent upon the amount of plastic deformation that can take place at the tip of a defect. In this regard the three following comments are made:

   (a) If linear elastic behaviour prevails, as defined by the validity conditions, the K_{IC} test applies. The accurate prediction of structural failure will depend on the precision in determining the applied stress, defect characterization and the K_{IC} value.

   (b) If general yielding takes place followed by abrupt fast fracture, the COD or J integral tests may apply. The critical COD value can be used directly to calculate the fracture stress or critical defect size. A reasonable agreement has been found between COD values measured from small laboratory specimens and large-scale wide plate and pressure vessels (the small specimens were lower by a factor of about 1.5).

   The J integral data can be used to calculate a valid K_{IC} number provided the test specimen geometry fulfills the validity requirements.

(c) When a material exhibits extensive plastic deformation and failure takes place by ductile crack extension followed by plastic collapse, all of the fracture mechanics techniques provide overly conservative predictions of the conditions for final failure. If the ductile material is to be used in a large section and a K_{IC} value is required, the J integral test performed on a small specimen may be converted to a valid K_{IC} number.

6. It is questionable whether dynamic fracture toughness K_{Id} data is relevant to the HAZ where dynamic loading is less likely to occur than in the base material.

In general, it remains to be proven that K_{Id} data measured from an instrumented Charpy test is comparable to that obtained from large specimens which exhibit linear elastic behaviour.

7. The Charpy test may be useful as a quality control test for comparing the HAZ toughness of various weldments, with the following reservations:

(a) If as-welded specimens are being tested, crack initiation and propagation must take place within the HAZ region. The test is invalid if the crack deviates from the HAZ.

(b) Simulated HAZ specimens, by providing a large area of uniform structure, allow the various regions of the HAZ to be evaluated by the Charpy test.

REFERENCES

1. Munse, W.H. "Brittle fracture in weldments"; Fracture, 4, p. 371; Academic Press; Ed. H. Liebowitz; 1969.

2. International Institute of Welding "Provisional Report on an international investigation of brittle fracture"; Doc. IX-407-64; 1964.

3. Kihara, H., Yoshida T. and Oba, H. "Initiation and propagation of brittle fracture in welded steel plate"; IIW Doc. X-217-59; 1959.

4. Dolby, R.E. and Archer, G.L. "The assessment of heat-affected zone fracture toughness"; Proc. of Conf. on Appl. of Fract. Mech. to Pressure Vessel Tech., Inst. Mech. Eng.; p. 190; 1971.

5. "Report on methods for fracture toughness tests for weldments"; IIW Doc. X-716-73; 1973.

6. Dolby, R.E. and Saunders, G.G. "Metallurgical factors controlling the heat-affected zone fracture toughness of C:Mn and low alloy steels"; IIW Doc. IX-891-74; 1974.

7. Dolby, R.E. and Saunders, G.G. "Sub-critical HAZ fracture toughness of C:Mn Steels"; Met. Const. and Brit. Weld. J., 4, p. 185; 1972.

8. Banks, E. "Toughness properties of HAZ structures in structural steel"; Welding J.; p. 299-s; July 1974.

9. Cane, M.W.F. and Dolby, R.E. "Metallurgical factors controlling the HAZ fracture toughness of submerged arc welded C-Mn steels"; Welding Research Inst.; 4, No. 3, p. 51; 1974.

10. Dolby, R.E. "The influence of defect orientation on heat affected zone fracture toughness measurements"; Met. Const. and Brit. Weld. J., 6, p. 228; 1974.

11. Dawes, M.G. "Testing for brittle fracture on low alloy QT steel weldments"; Met. Const., 2, p. 533; 1970.

12. Knott, J.K. "Fundamentals of fracture mechanics"; London, Butterworths; 1973.

13. Dolby, R.E. "Fracture toughness comparison of weld HAZ and thermally simulated microstructures"; Research Application Seminar, Weld Thermal Simulators for Research and Problem Solving, The Welding Institute; 1972.

14. "Plane strain fracture toughness of metallic materials"; ASTM Std. E399.

15. Wells, A.A. "Unstable crack propagation in metals, cleavage and fast fracture"; Cranfield Propagation Symposium, p. 210; 1961.

16. "Fracture toughness testing of metallic materials -- Part II -- COD testing"; Brit. Stds. Assoc. DD19; 1972.

17. Barr, R.R., Elliott, D., Terry, P. and Walker, E.F. "The measurement of COD and its application to defect significance"; Met. Const., p. 604; Dec. 1975.

18. Griffis, C.A. "Elastic plastic fracture toughness: A comparison of J integral and crack opening displacement characterization"; Trans. ASME, J. of Press. Vess. Tech.; p. 278; Nov. 1975.

19. Rice, J.R. "A path independent integral and the approximate analysis of strain concentration by notches and cracks"; Trans. ASME, Ser. E., J. of App. Mech. 35, p. 379; 1968.

20. Landes, J.D. and Begley, J.A. "Test results from J integral studies: An attempt to establish a J_{IC} testing procedure"; ASTM STP560, p. 170; 1973.

21. Begley, J.A. and Landes, J.D. "The J integral as a fracture criterion"; ASTM, STP 514, p. 1; 1972.

22. "Impact testing of metals"; ASTM STP 466; 1969.

23. "Instrumented impact testing"; ASTM STP 563; 1973.

24. "Dynamic testing - The proposed specifications"; Met. Const.; p. 473; Sept. 1975.

25. Matthews, W.T. "The role of impact testing in characterizing the toughness of materials"; ASTM STP 466, p. 3; 1969.

26. "Drop-weight tear tests of ferritic steels"; ASTM Std. E436.

27. Smith, E. and Patchett, B.M. "Effects of notch acuity and side grooving on fracture toughness"; Welding J.; p. 169-s; June 1975.

28. Banks, E.E. "A fracture mechanics assessment of the HAZ properties of Australian structural steels"; Aust. Welding J., p. 59; Sept./Oct. 1974.

29. Goldak, J.A. and Nguyen, D.S. "A fundamental difficulty in notch toughness testing narrow welds and HAZ"; Carleton Univ. Rep.; Sept. 1975.

30. Taniguchi, N., Yamato, K., Nakashima, A., Minami, K. and Kanazawa, S. "Toughness near the fine grained fusion line of HSS developed for high heat input welding"; Proc. of Jap. U.S. Sem. Signif. of Defects in Weld. Struct.; 1973.

31. Ivens, P.F. and Van den Bergh, A.A. "Impact testing of the HAZ"; Met. Const. and Brit. Weld. J., p. 234; July 1974.

32. Ivens, P.F. and Van den Bergh, A.A. "Toughness of the HAZ of welds in C and C-Mn steels"; IIW Doc. IX-903-74; 1974.

33. Schofield, R. and Weiner, R.T. "Simulating HAZ toughness in pipeline steels"; Met. Const. and Brit. Welding J.; p. 45; Feb. 1974.

34. Grover, H.K. and Jolley, G. "Fracture characteristics of simulated HAZ's in a low-alloy constructional steel"; Met. Const. and Brit. Welding J., p. 2; July 1974.

35. Wessel, E.T. and Mager, T.R. "Fracture mechanics technology as applied to thick-walled nuclear pressure vessels"; Proc. of Conf. on Appl. of Fract. Mech. to Press. Vessel Tech., Instn. Mech. Eng., p. 17; 1971.

36. Rolfe, S.T. "Use of fracture mechanics in design"; Int. Met. Rev. 19, p. 183; 1974.

37. Egan, G.R. "The application of fracture toughness data to the assessment of pressure vessel integrity"; ASME, 2nd Int. Conf. on Pressure Vessel Tech., Vol. II, p. 1037; 1973.

38. Kirby, N., Ingham, T. and Cowan, A. "The use of COD as a measure of fracture initiation on steel pressure vessels"; ASME, 2nd Int. Conf. on Pressure Vessel Tech., Vol. II, p. 943; 1973.

39. Cowan, A. and Kirby, N. "The application of COD measurements to large scale test behaviour"; Prac. Fract. Mech. for Struct. Steel, U.K. Atom. Energy Auth.; p. D1; 1969.

40. Fearnehough, G.D., Lees, G.M., Lowes, J.M. and Weiner, R.T. "The role of stable ductile crack growth in the failure of structures"; Proc. of Conf. on Appl. of Fract. Mech. to Pressure Vessel Tech., Instn. Mech. Eng., p. 119; 1971.

41. Weiss, B.Z., Steffens, H.D., Seifert, K. and Staskewitsch, E.S. "Dynamic fracture instability in welded 17-7 PH type steel by instrumented impact tests"; Welding J., p. 216-s; July 1975.

42. Server, W.L. and Tetelman, A.S. "The use of pre-cracked Charpy specimens to determine dynamic fracture toughness"; Eng. Fract. Mech. 4, p. 367; 1972.

TABLE 1

COD Test Results for Series T and U Specimens (10)

Series	Test Temperature °C	Critical COD mm
T	+16	1.3 (maximum load)
T	-80	0.56
T	-80	0.58
U	+16	1.5 (maximum load)
U	-80	0.14
U	-80	0.12
U but notched in weld deposit	-80	0.11

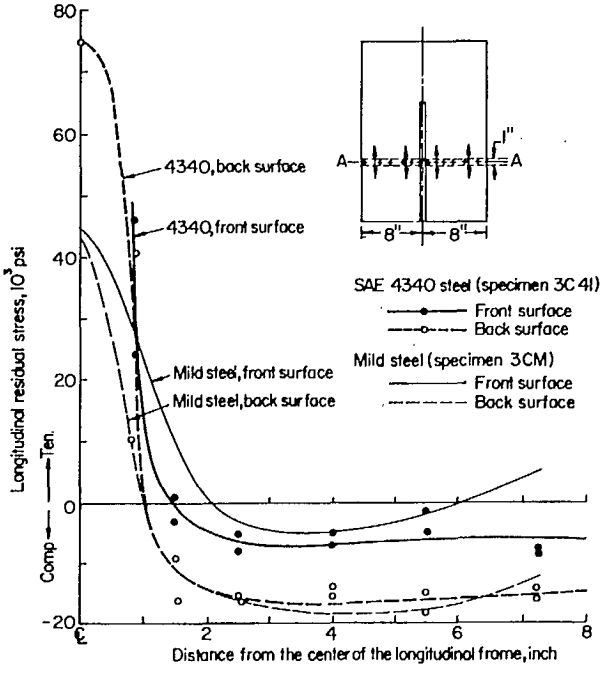

Fig. 1 - Distributions of longitudinal residual stresses in welded plate[1]

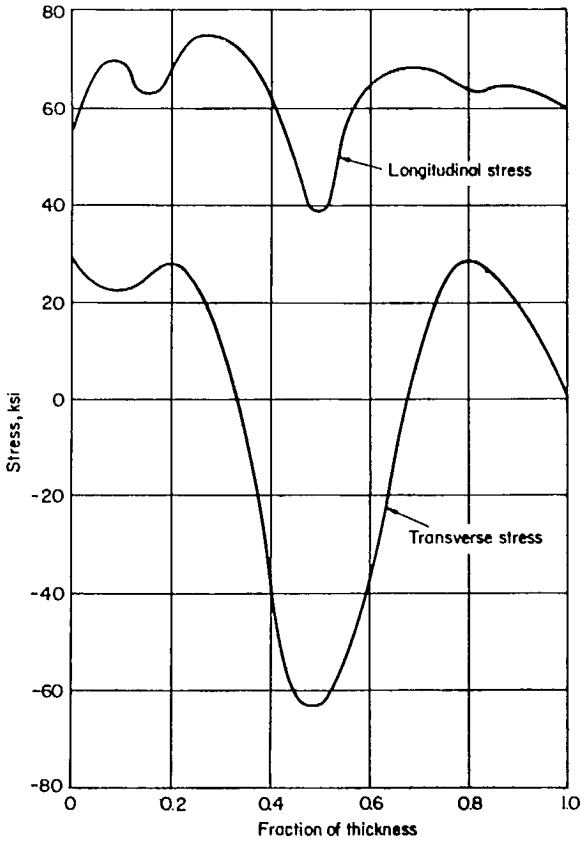

Fig. 2 - Distribution of residual stress through thickness of a weld in 1 inch thick as-welded specimen[1]

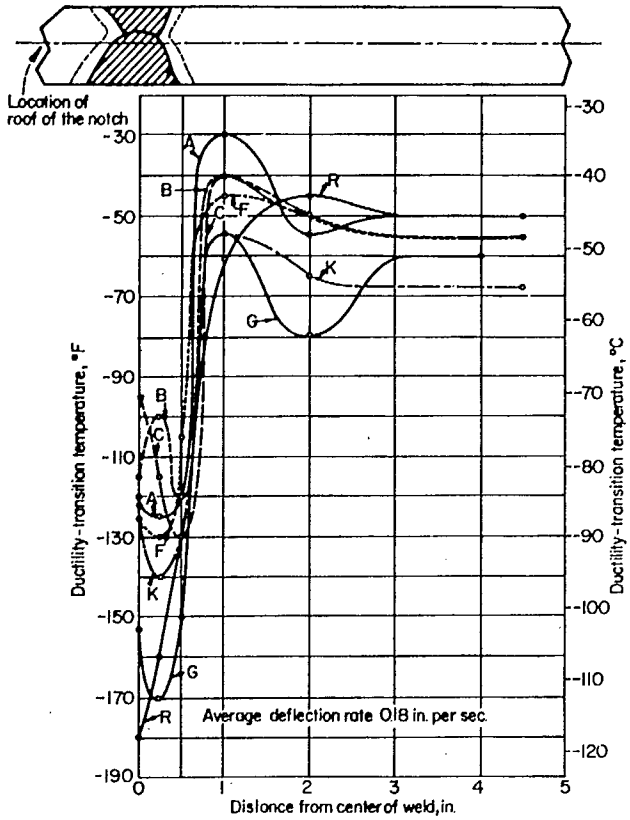

Code	Type of steel	C	Mn	Si	V	Ti
A	C(semikilled)	0.23	0.48	0.05	—	—
B	C-Mn	0.18	1.09	0.16	—	—
C	Mn-V-Ti	0.11	1.03	0.26	0.03	0.01
F	C (fully killed)	0.23	0.53	0.19	—	—
G	C (fully killed)	0.20	0.61	0.21	—	—
K	C (fully killed)	0.13	0.42	0.22	—	—
R	C (rimmed)	0.23	0.47	0.004	—	—

Fig. 3 - Variation of the toughness from centre of a butt weld to the base metal for carbon steel weldments[1]

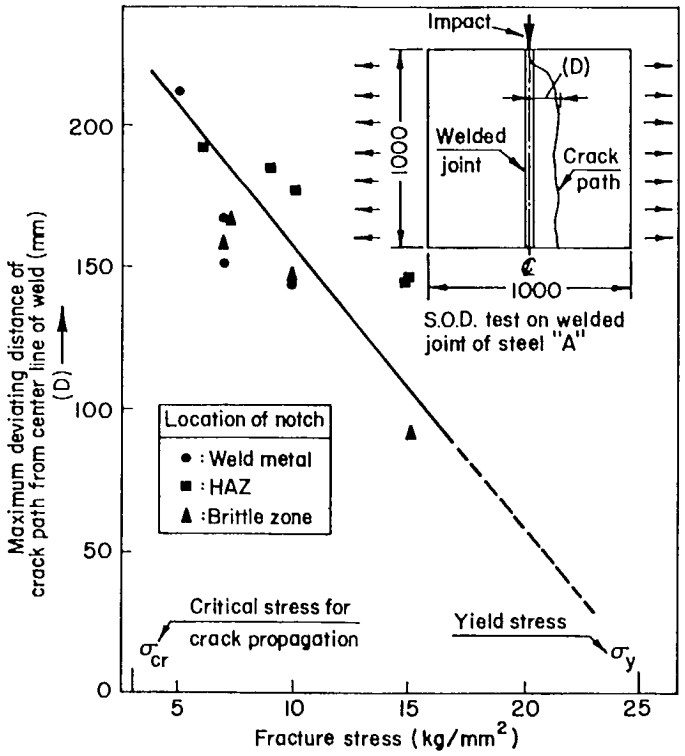

Fig. 4 - Relation between fracture stress and deviation of crack from notch line[3]

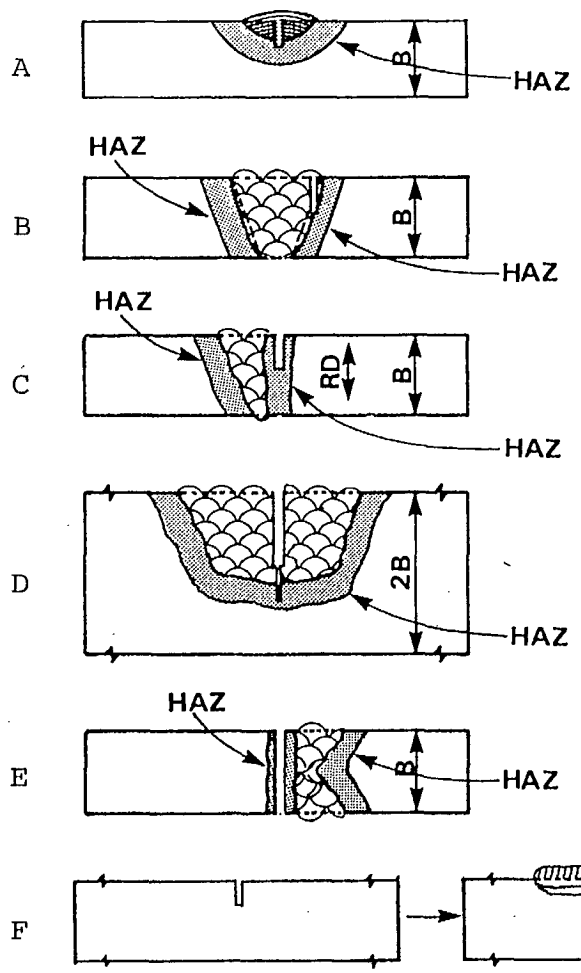

	Thick.	Width	Notch Depth / Spec. Width
A	B	B	Depends on Bead Penet.
B	B	B	.3
C	B	B	.3
D	B	2B	.5
E	B	2B	.5

Fig. 5 - Specimen designs for assessing HAZ fracture toughness[4]

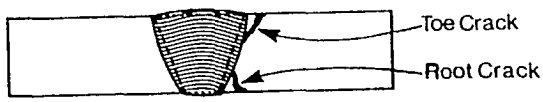

Fig. 6 - Longitudinal toe and root HAZ cracks

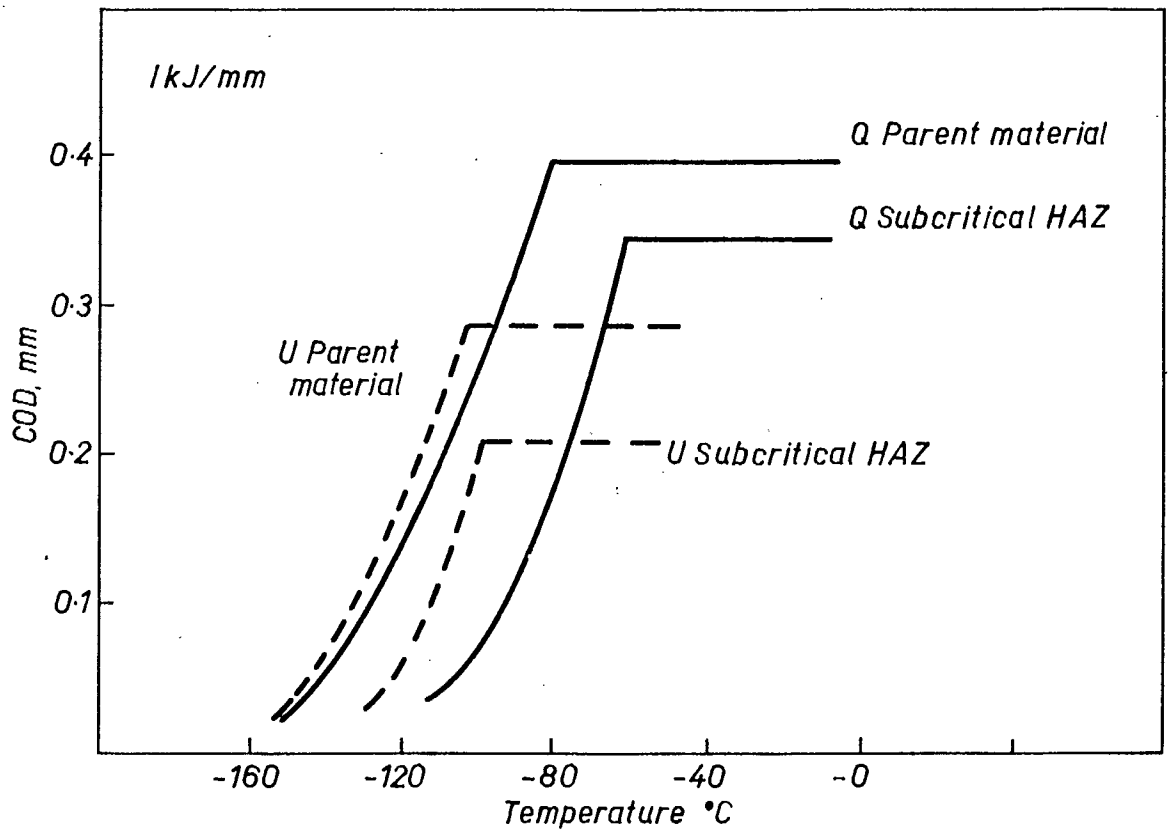

Fig. 7 - Fracture toughness in sub-critical HAZ region[6]

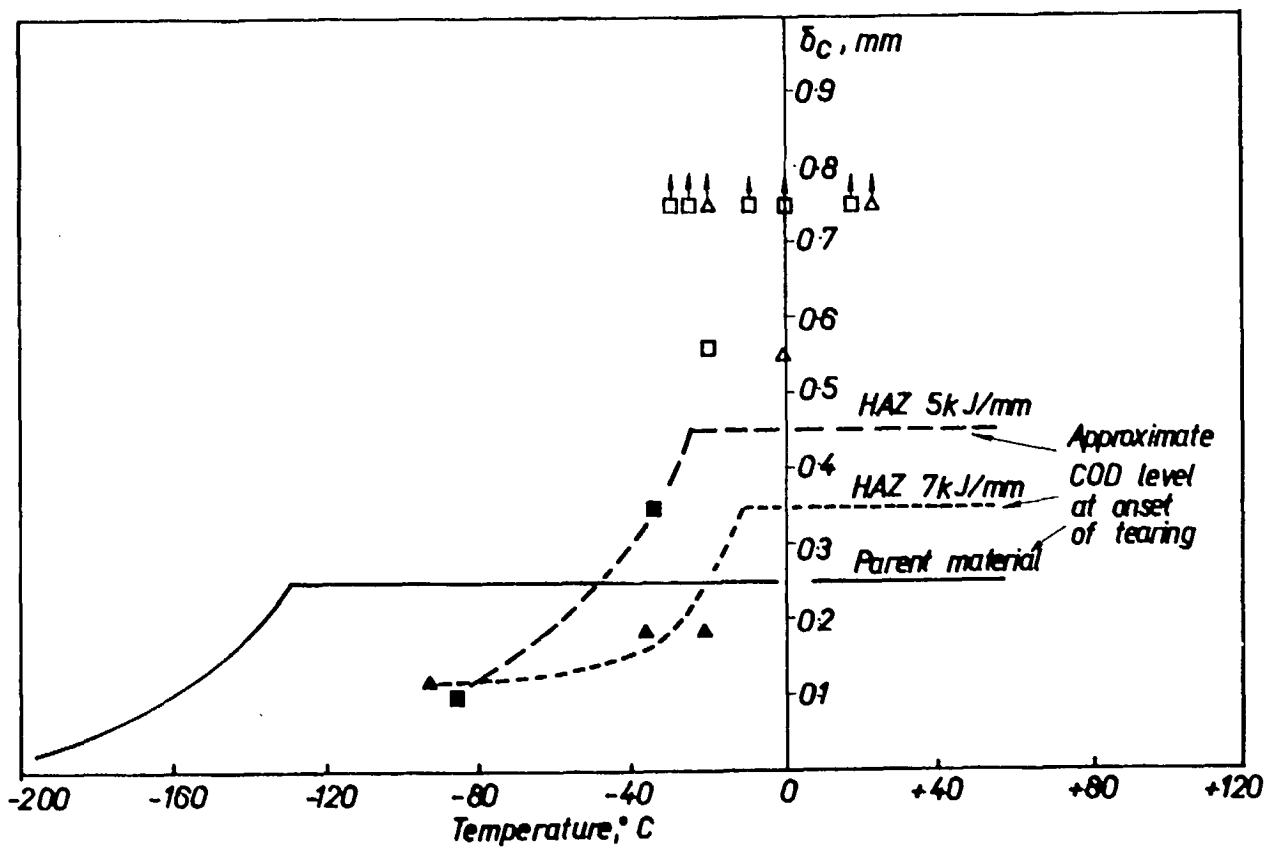

Fig. 8 - COD transition curves for grain coarsened HAZs; open symbols refer to fracture by ductile tearing[9]

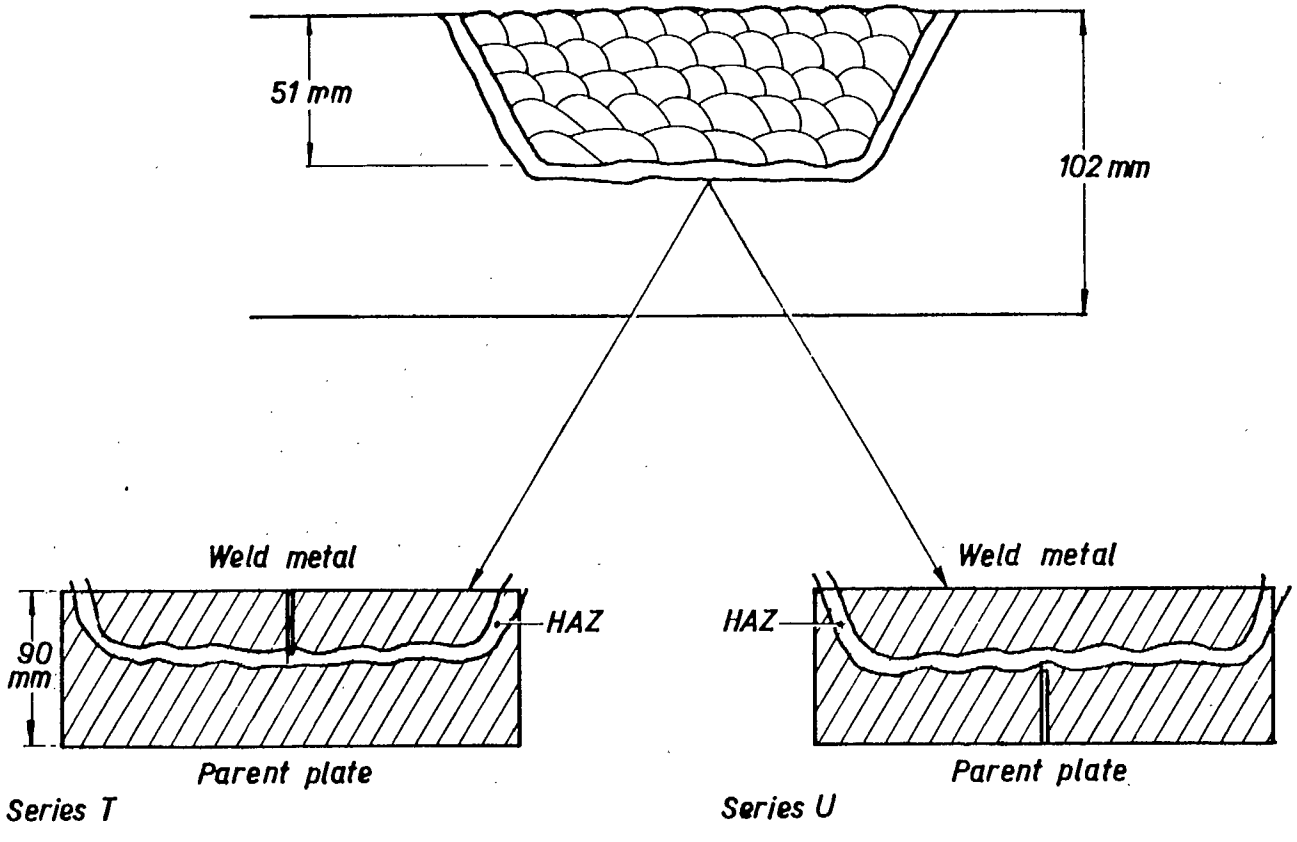

Fig. 9 - Notching positions in HAZ fracture toughness specimens[10]

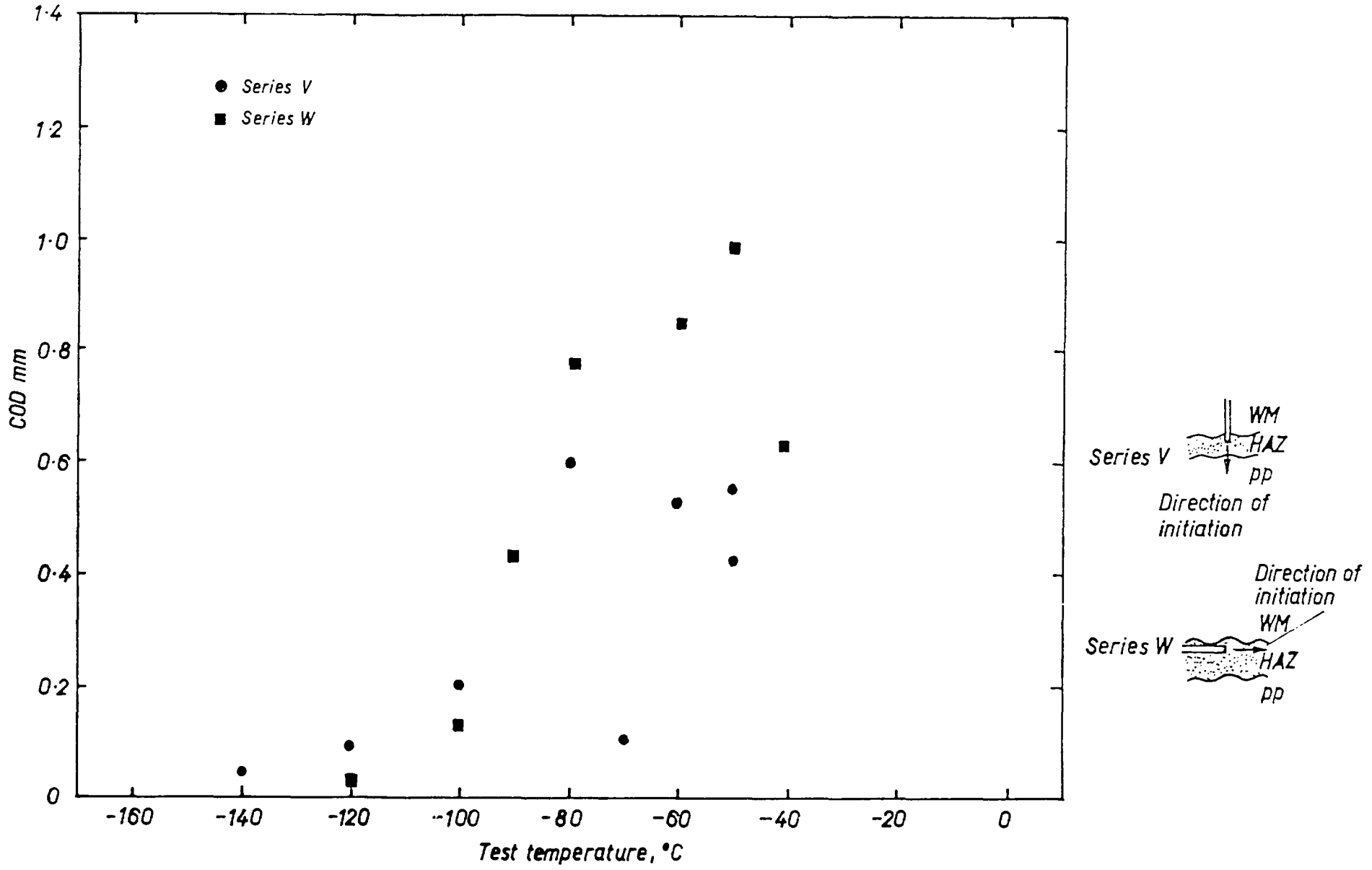

Fig. 10 - Effect of notch orientation on the HAZ fracture toughness of a C:Mn steel[10]

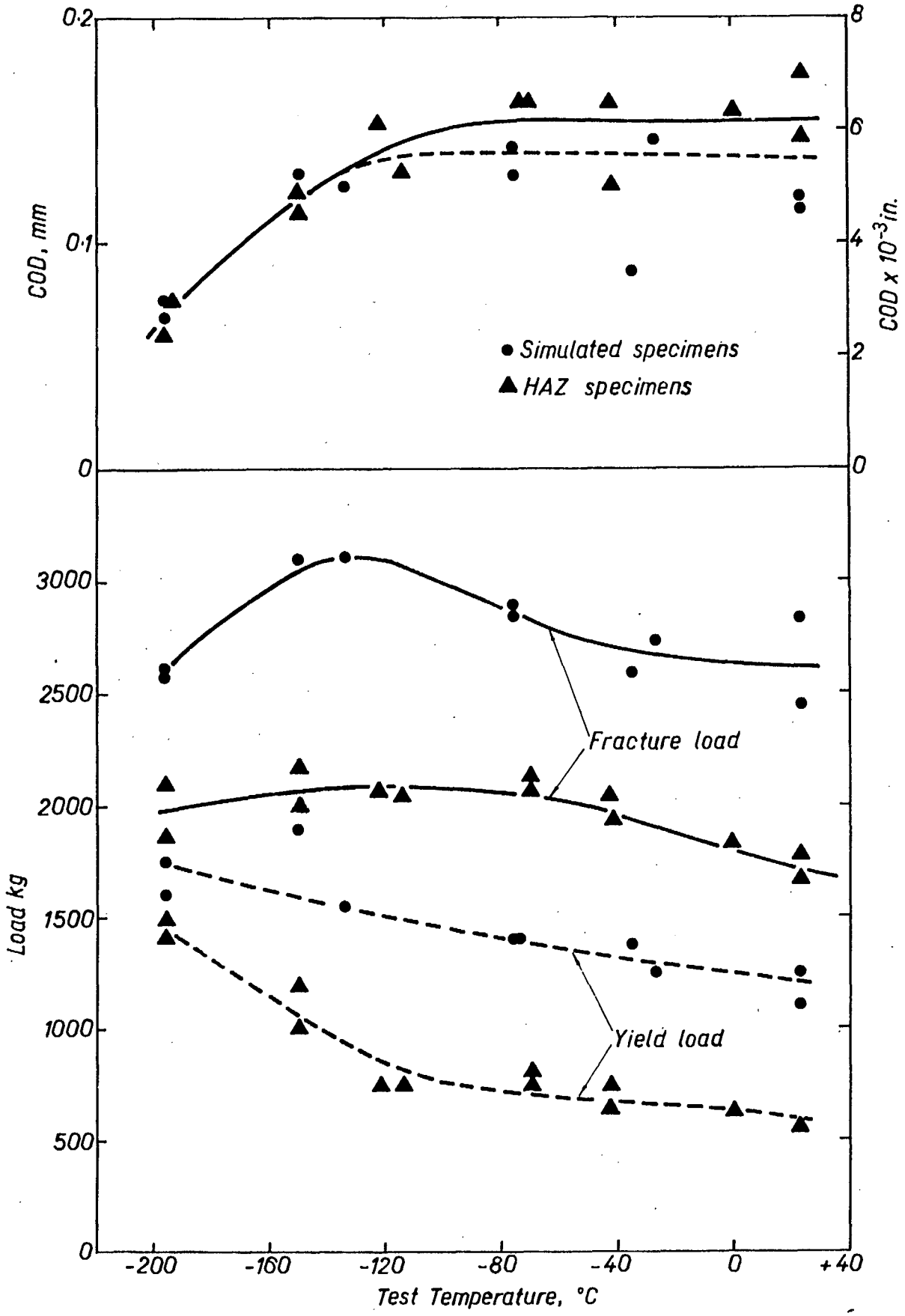

Fig. 11 - Test results for simulated and weld HAZ specimens. Grain coarsened region[13]

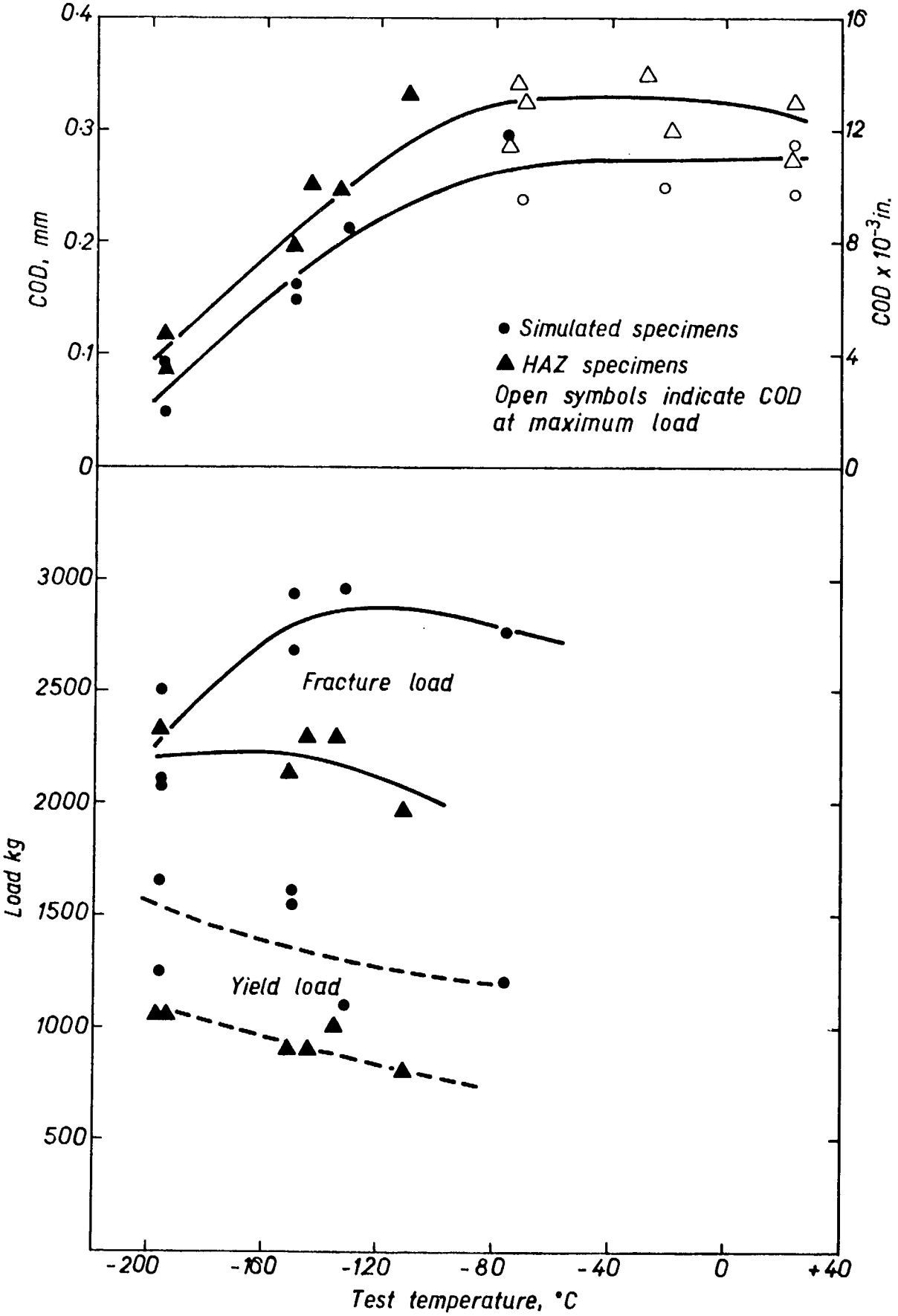

Fig. 12 - Test results for simulated and weld HAZ specimens. Grain refined region[13]

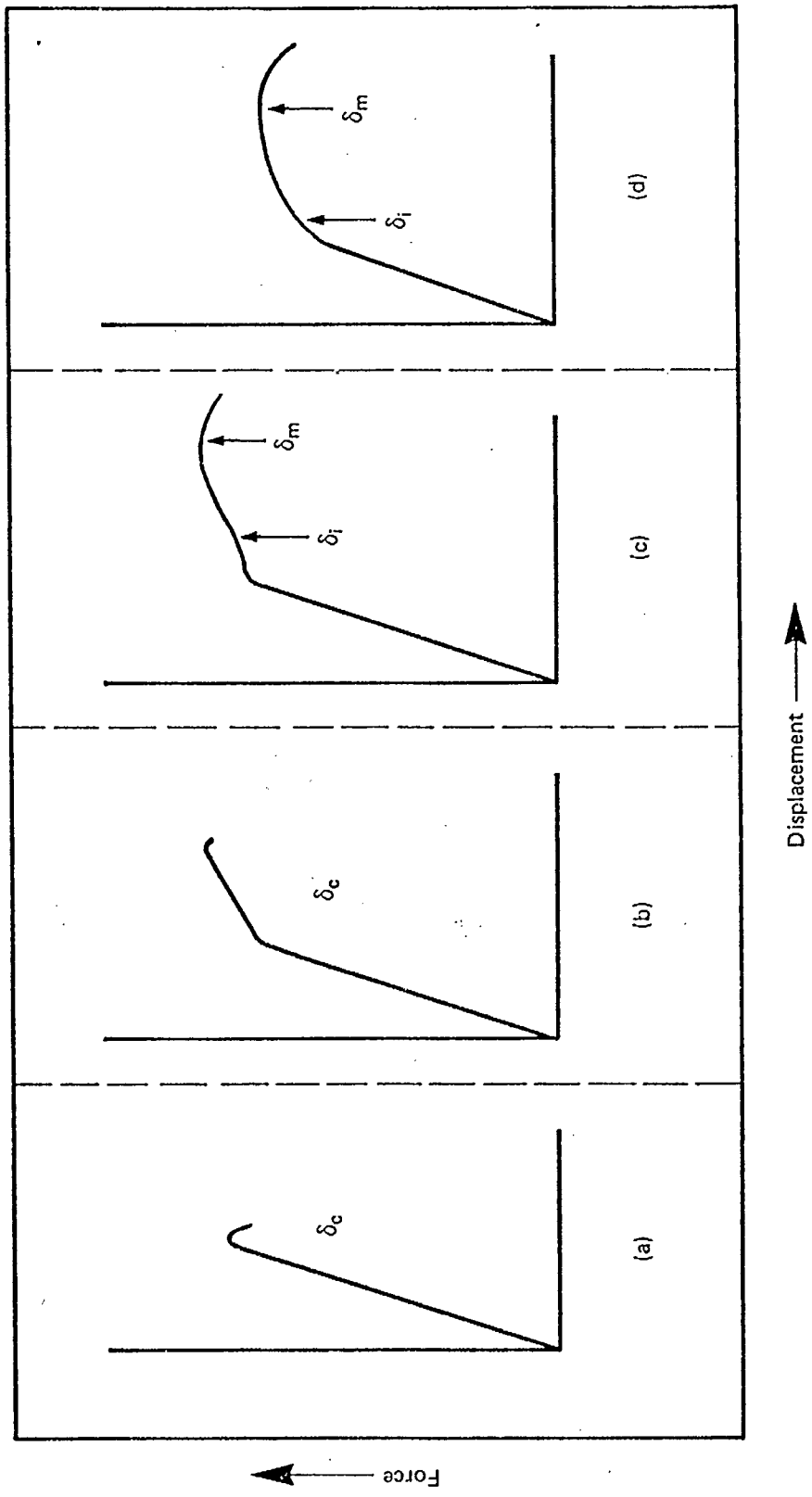

Fig. 13 - COD force/displacement diagrams[17]

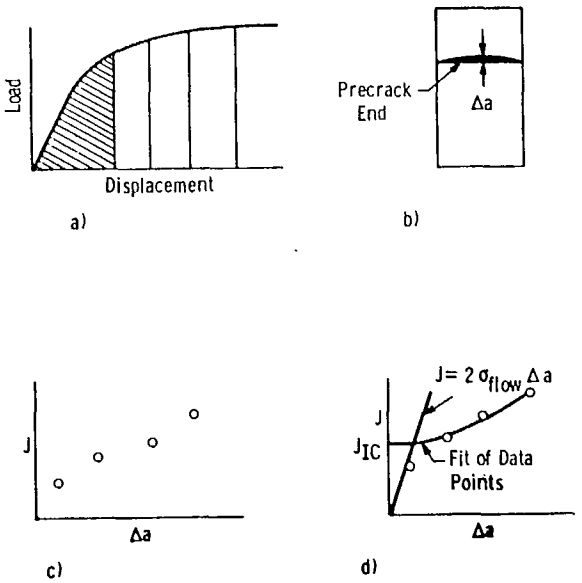

Fig. 14 - Procedure for J_{IC} measurement[20]
(a) load specimens to various displacements
(b) measure crack extension
(c) plot J vs. Δ a
(d) determination of J_{IC}

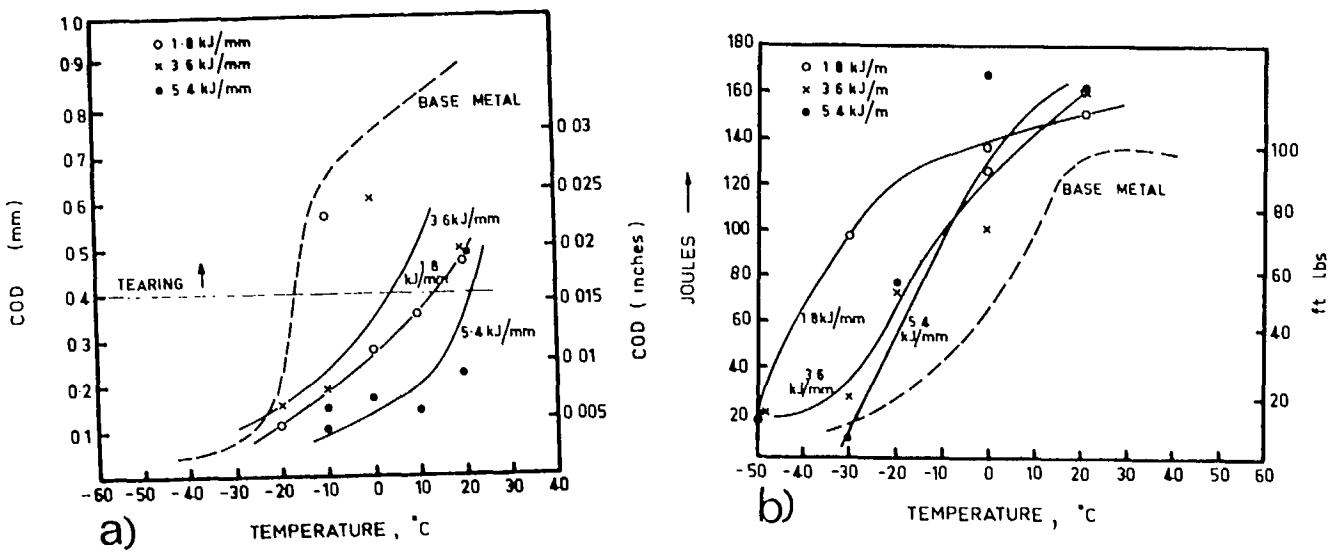

Fig. 15 - (a) COD results for HAZ as a function of heat input[28]
(b) Charpy impact results for HAZ[28]

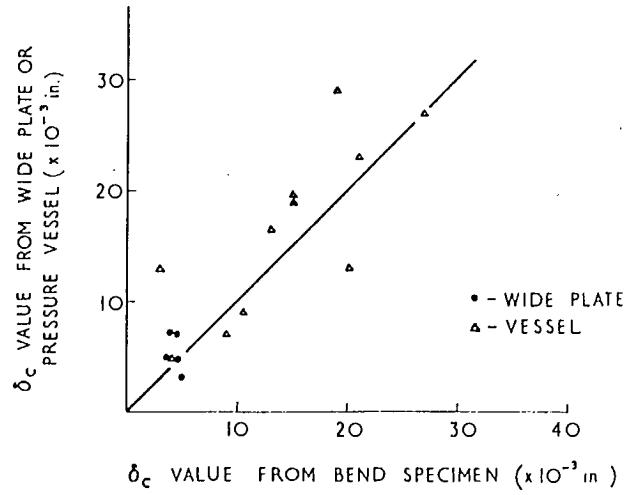

Fig. 16 - Comparison of critical COD's measured on bend specimens with corresponding values from wide plates and pressure vessels(38)

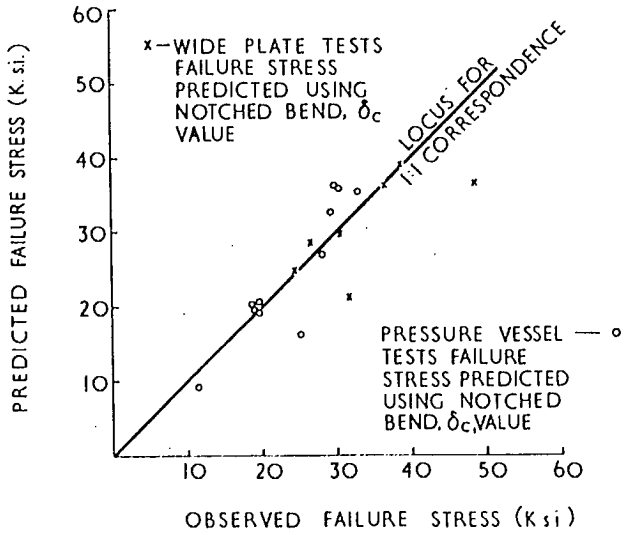

Fig. 17 - Comparison of predicted and measured failure stresses for wide plates and pressure vessels(38)

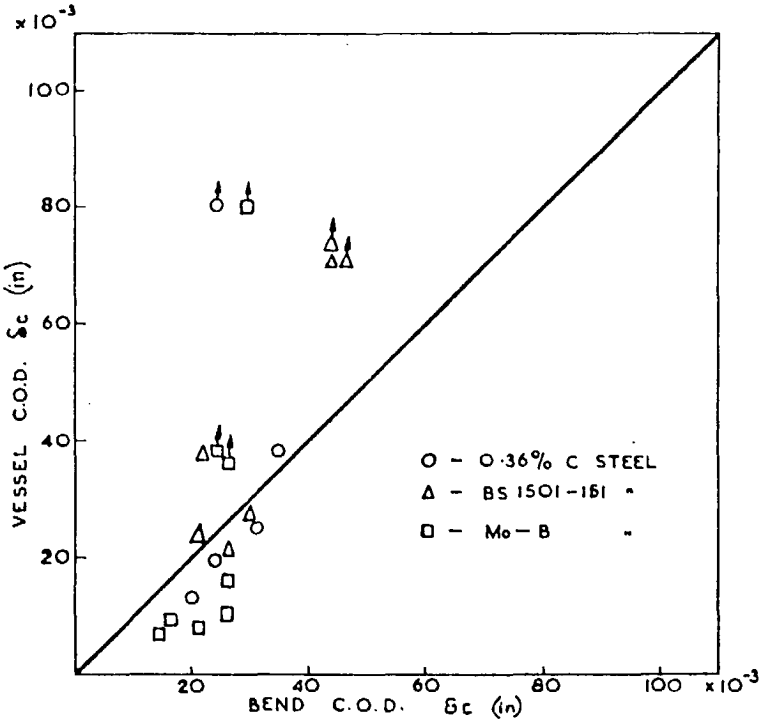

Fig. 18 - Comparison of critical COD's from vessels and bend specimens[39]

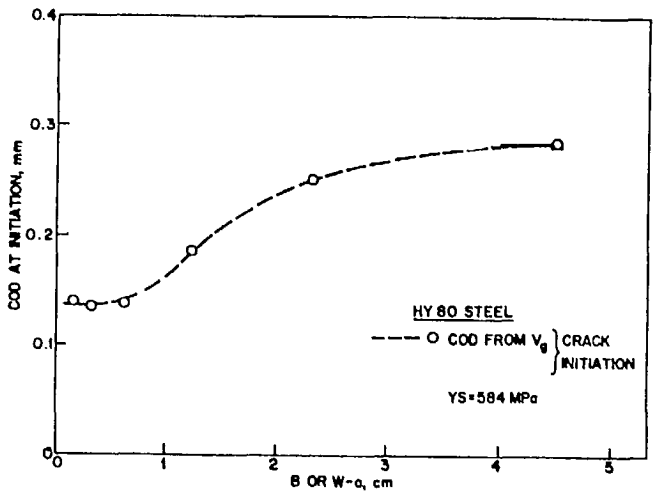

Fig. 19 - Effect of specimen size on COD at initiation[18]

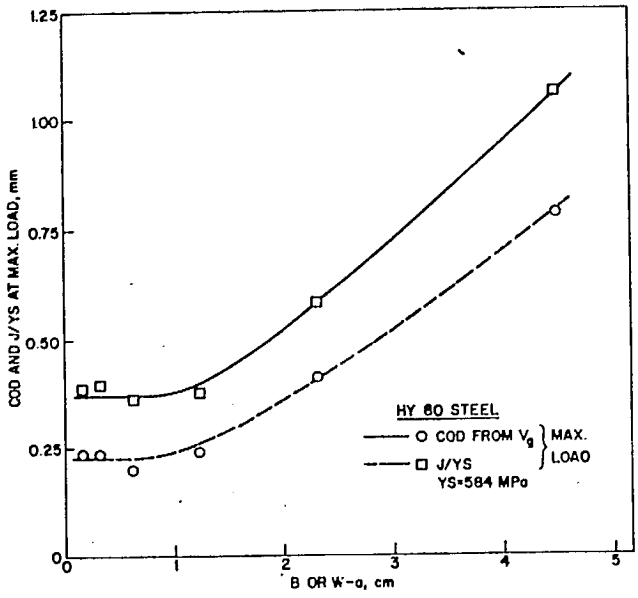

Fig. 20 - Specimen size dependence of COD and $J/_{ys}$ determined at maximum load[18]

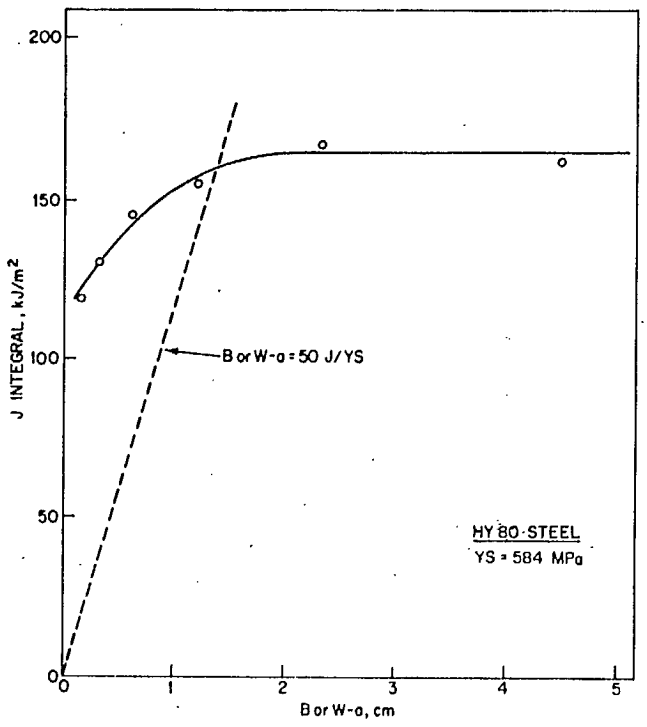

Fig. 21 - Effect of specimen size on J integral at initial crack extension[18]

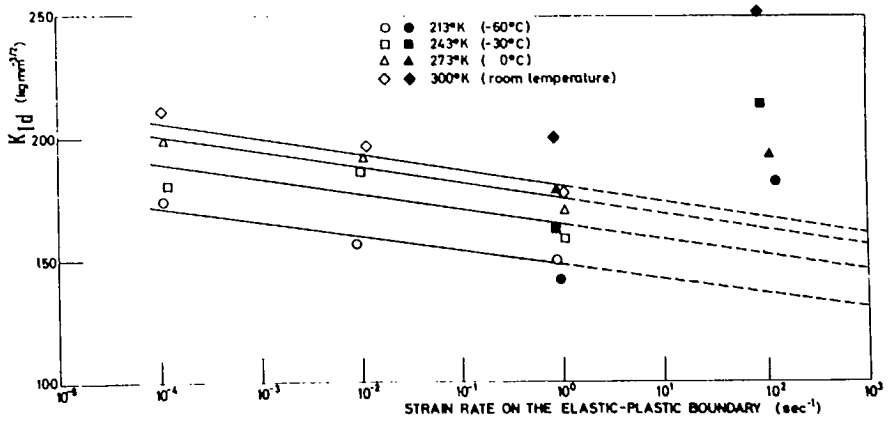

Fig. 22 - Effect of temperature and strain rate on K_{Id} of 17-7 PH stainless steel. White points, large specimens; black points, small Charpy specimens(29)

APPENDIX I

ECONOMICS OF FRACTURE TESTING

The following is a breakdown of the costs involved in performing the various fracture mechanics and impact tests. A labour cost factor of $18 per hour including 100% overhead was used in all calculations:

TASK	TIME(minutes)
K_{IC} Test	
1. Preparation of notched specimen	
(a) bend specimen	150
(b) compact tension specimen	300
2. Fatigue precracking	90
3. Static loading to failure	10
4. Calculation of K_{IC}	
(a) measurement of fatigue crack	20
(b) calculation of K_{IC} from appropriate data	20

Three specimens are required

Therefore total cost = $260 (bend specimen)

= $400 (compact tension specimen)

NOTE: The cost of the COD test should be equivalent to the K_{IC} test.

J Integral Test	
1. Preparation of notched specimen	
(a) bend specimen	150
(b) compact tension specimen	300
2. Fatigue precracking	90

3. Static loading to failure	10
4. Measurement of crack front displacement, Δ a	
(a) heat tinting and fracture	10
(b) measurement of crack front	20
5. Calculation of J_{IC}	
(a) determination of area under load/displacement curve	15
(b) plotting of J vs Δa curve	20

Five specimens are required
Therefore total cost = \$470 (bend specimen)
= \$700 (compact tension specimen)

K_{Id} Test

1. Preparation of notched specimen	60
2. Fatigue precracking	90
3. Impact loading to failure	10
4. Calculation of K_{Id}	
(a) measurement of fatigue crack	20
(b) calculation of K_{Id} from appropriate data	20

Three specimens are required
Therefore total cost = \$180

Charpy Impact Test

1. Preparation of notched specimen	60

2. Impact loading and fracture surface measurement

(a)	at room temperature	15
(b)	at other than room temperature	20

Fifteen specimens are required for transition curve
Therefore total cost = $355

CANMET REPORTS

Recent CANMET reports presently available or soon to be released through Printing and Publishing, Supply and Services, Canada (addresses on inside front cover), or from CANMET Publications Office, 555 Booth Street, Ottawa, Ontario, K1A 0G1:

Les récents rapports de CANMET, qui sont présentement disponibles ou qui ce seront bientôt, peuvent être obtenus de la direction de l'Imprimerie et de l'Edition, Approvisionnements et Services, Canada (adresses au verso de la page couverture), ou du Bureau de Vente et distribution de CANMET, 555 rue Booth, Ottawa, Ontario, K1A 0G1:

77-9 Filtration - Filters and filter media; H.A. Hamza;
Cat. No. M38-13/77-9, ISBN 0-660-01174-3; Price: $2.00 Canada, $2.40 other countries.

77-11 Ozonation for destruction of cyanide in Canadian gold mill effluents - A preliminary evaluation; G.I. Mathieu;
Cat. No. M38-13/77-11, ISBN 0-660-01171-9; Price: $1.50 Canada, $1.80 other countries.

77-12 Pit slope manual - Chapter 3 - Mechanical properties; M. Gyenge and G. Herget;
Cat. No. M38-14/3-1977, ISBN 0-660-00994-3; Price: $3.50 Canada, $4.20 other countries.

77-13 Pit slope manual - Chapter 4 - Groundwater; J. Sharp, G. Ley and R. Sage;
Cat. No. M38-14/4-1977, ISBN 0-660-01006-2; Price: $3.25 Canada, $3.90 other countries.

77-15 Pit slope manual - Chapter 8 - Monitoring; G. Larocque;
Cat. No. M38-14/8-1977, ISBN 0-660-01012-7; Price: $3.50 Canada, $4.20 other countries.

77-22 Pit slope manual - Supplement 2-3 - Geophysics for open pit sites; G. Herget;
Cat. No. M38-14/2-1977-3, ISBN 0-660-00991-9; Price: $2.50 Canada, $3.00 other countries.

77-36 Thermal hydrocracking of Athabasca bitumen: Effect of recycle-gas purity on product yields and qualities; A.M. Shah, B.B. Pruden and J.M. Denis;
Cat. No. M38-13/77-36, ISBN 0-660-01172-7; Price: $1.25 Canada, $1.50 other countries.

77-38 Comparison of notch-ductility and weldability of three high-strength structural steels; W.P. Campbell;
Cat. No. M38-13/77-38, ISBN 0-660-01217-0; Price: $2.00 Canada, $2.40 other countries.

77-39 The environmental cracking susceptibilities of three high-strength alloy steels; G.J. Biefer;
Cat. No. M38-13/77-39, ISBN 0-660-01242-1; Price: $1.00 Canada, $1.20 other countries.

77-42 Maturation studies on Canadian east coast oils; H. Sawatzky, A.E. George, R.C. Banerjee, G.T. Smiley and O.S. Montgomery;
Cat. No. M38-13/77-42, ISBN 0-660-01206-5; Price: $1.00 Canada, $1.20 other countries.

77-44 Thermal hydrocracking of Athabasca bitumen: Steady-state effects on product yields and qualities in the absence of scrubbing of the recycle gas; A.M. Shah, B.B. Pruden and J.M. Denis;
Cat. No. M38-13/77-44, ISBN 0-660-01241-3; Price: $1.00 Canada, $1.20 other countries.

77-45 Exploratory corrosion tests in the Canadian Arctic; G.J. Biefer;
Cat. No. M38-13/77-45, ISBN 0-660-01416-5; Price: $1.00 Canada, $1.20 other countries.

77-46 Comparison of coke produced in different CANMET coke ovens: Part 1: 12- and 18-inch oven coke strengths; W.R. Leeder and J.T. Price;
Cat. No. M38-13/77-46, ISBN 0-660-01194-8; Price: $1.25 Canada, $1.50 other countries.

77-49 Effect of elevated temperatures on compressive strength, pulse velocity and conversion of high alumina cement concrete; O.H.H. Quon and V.M. Malhotra;
Cat. No. M38-13/77-49, ISBN 0-660-01436-X; Price: $2.25 Canada, $2.70 other countries.

77-50 A comparative study of Fe catalysts, $ZnCl_2$ catalysts and $ZnCl_2$ - Promoted Fe catalysts for hydrocracking of Athabasca bitumen; W.A.O. Herrmann, L.P. Mysak and K. Belinko;
Cat. No. M38-13/77-50, ISBN 0-660-01218-9; Price: $0.75 Canada, $0.90 other countries.

77-51 Analysis of reactor samples collected during thermal hydrocracking of Athabasca bitumen; K. Belinko and J.M. Denis;
Cat. No. M38-13/77-51, ISBN 0-660-01245-6; Price: $1.00 Canada, $1.20 other countries.